HHS Public Access

Author manuscript

Cell Mol Bioeng. Author manuscript; available in PMC 2017 March 01.

Published in final edited form as:

Cell Mol Bioeng. 2016 March 1; 9(1): 38–54. doi:10.1007/s12195-015-0423-6.

Poly(ethylene glycol) Hydrogel Scaffolds Containing Cell-Adhesive and Protease-Sensitive Peptides Support Microvessel Formation by Endothelial Progenitor Cells

Erica B. Peters, Ph.D.,
Fitzpatrick CIEMAS Building, Room 1427, Box 90281, Duke University, Department of Biomedical Engineering, Durham, NC 27708

Nicolas Christoforou, Ph.D.,
P.O. Box 127788, Khalifa University, Department of Biomedical Engineering, Abu Dhabi, UAE

Kam W. Leong, Ph.D.,
1210 Amsterdam Avenue, Mail Code 8904, Columbia University, Department of Biomedical Engineering, New York, NY 10027

George A. Truskey, Ph.D., and
Fitzpatrick CIEMAS Building, Room 1427, Box 90281, Duke University, Department of Biomedical Engineering, Durham, NC 27708

Jennifer L. West, Ph.D.
Fitzpatrick CIEMAS Building, Room 1427, Box 90281, Duke University, Department of Biomedical Engineering, Durham, NC 27708

Erica B. Peters: ecb22@duke.edu; Nicolas Christoforou: nicolas.christoforou@kustar.ac.ae; Kam W. Leong: kwl2121@columbia.edu; George A. Truskey: george.truskey@duke.edu; Jennifer L. West: jennifer.l.west@duke.edu

Abstract

The development of stable, functional microvessels remains an important obstacle to overcome for tissue engineered organs and treatment of ischemia. Endothelial progenitor cells (EPCs) are a promising cell source for vascular tissue engineering as they are readily obtainable and carry the potential to differentiate towards all endothelial phenotypes. The aim of this study was to investigate the ability of human umbilical cord blood-derived EPCs to form vessel-like structures within a tissue engineering scaffold material, a cell-adhesive and proteolytically degradable poly(ethylene glycol) (PEG) hydrogel. EPCs in co-culture with angiogenic mural cells were encapsulated in hydrogel scaffolds by mixing with polymeric precursors and using a mild photocrosslinking process to form hydrogels with homogeneously dispersed cells. EPCs formed 3D microvessels networks that were stable for at least 30 days in culture, without the need for supplemental angiogenic growth factors. These 3D EPC microvessels displayed aspects of

Correspondence to: Erica B. Peters, ecb22@duke.edu.

Conflicts of Interest

Erica B. Peters, Nicolas Christoforou, Kam W. Leong, George A. Truskey, and Jennifer L. West declare that they have no conflicts of interest.

Ethical Standards

No human or animal studies were carried out by the authors of this article.

physiological microvasculature with lumen formation, expression of endothelial cell proteins (connexin 32, VE-cadherin, eNOS), basement membrane formation with collagen IV and laminin, perivascular investment of PDGFR-β and α-SMA positive cells, and EPC quiescence (<1% proliferating cells) by 2 weeks of co-culture. Our findings demonstrate the development of a novel, reductionist system that is well-defined and reproducible for studying progenitor cell-driven microvessel formation.

Introduction

Vascularization remains a key challenge in the field of regenerative medicine due to the complexity of recapitulating *in vivo* processes of capillary formation to produce functional, stable microvasculature [1–2]. *In vivo*, microvessels are formed from pre-existing microvessels (angiogenesis) in response to injury, or *de novo*, during embryonic development, from endothelial progenitor cells (EPCs) (vasculogenesis) [3–4]. For both angiogenic and vasculogenic processes, the stages of microvessel formation require the coordinated actions of cytokine secretion, endothelial cell (EC) migration, lumen formation, extracellular matrix remodeling, and recruitment of mural cells [3–4]. Once recruited, the mural cells, including pericytes and vascular smooth muscle cells (SMCs), form intimate associations with ECs that provide structural support for nascent capillary vessels and protect against pathological microvessel growth by promoting quiescence of ECs [5–6]. Developing microvessels can also recruit mesenchymal stem cells (MSCs), which differentiate to mural cells upon contact with ECs through gap-junction channels [7–8].

One approach to developing microvasculature within tissue engineering scaffolds is to simulate *in vivo* microvessel formation conditions *in vitro*. This is possible through the combination of ECs and mural cells under pro-angiogenic conditions, such as the inclusion of vascular endothelial growth factor type A (VEGF-A) in culture media [1–2, 9–10]. A number of *in vivo* studies have also demonstrated that pre-formed, tissue engineered microvessels can anastomose with host vasculature and support perfusion [11–15]. Additionally, microvessels tissue engineered *in vitro* show promise as a therapeutic device for the vascularization of ischemic tissues [16].

Before translation of the tissue engineered microvessels to vascularization therapies can occur, all components of the system, which include vascular cells, biomaterials, and culture media conditions, must be rendered clinically acceptable. For instance, the use of vascular-derived ECs requires an invasive isolation procedure for the patient. An alternative, minimally invasive, source for ECs are EPCs, isolated from the peripheral blood of adults or umbilical cord blood [17]. These blood-derived EPCs, distinguished from mature ECs by increased expression of CD34+ and CD133+ hematopoietic progenitor cell markers [18], have demonstrated encouraging therapeutic potential with participation in neovascularization of angiogenic sites [19]. ECs derived from umbilical cord blood EPCs (hCB-EPCs) have extensive expansion potential, yielding near 10^{15}-fold expansion over 100 days of culture. As well, hCB-EPCs can be cryogenically preserved without appreciable loss in viability of CD34+, CD133+ cells and matched to non-autologous donors through human leukocyte-antigen (HLA)-typing [20–21]. hCB-EPCs have demonstrated vasculogenic

activity *in vivo* after combining with SMCs in Matrigel™ and injected subcutaneously on the backs of athymic mice to form lumenized microvessels that perfused within 1 week of implantation [22]. In comparison to adult peripheral blood-derived EPCs, hCB-EPCs are more genetically stable, evidenced by their significantly higher telomerase activity [17]. High telomerase activity is correlated with improved vasculogenic potential *in vivo* [23] and maintenance of stem cell differentiation potential after long-term expansion *in vitro* [24]. For these reasons, hCB-EPCs may offer the advantages over other EPC sources of enhanced *in vivo* microvessel formation and greater potential to differentiate towards tissue-specific endothelium. The hCB-EPCs may also provide an easier translational path as an "off-the-shelf" allogenic EC source than vascular-derived ECs or other potential stem cell sources, like induced pluripotent stem cells, where differentiation to ECs may be harder to control.

Despite their participation in neovascularization, EPCs require the support of mural cells to develop and maintain microvessel structures *de novo* [25–29], as do most types of differentiated ECs. We have previously shown co-culture of SMCs with ECs results in a self-sustainable angiogenic microenvironment, conducive for robust, stable microvessel growth with minimal supplemental growth factors [26–27]. This property is valuable because the use of supplemental growth factors may not be available upon implantation *in vivo*, potentially causing regression of microvessels. In addition, angiogenic cytokines can interfere with the development of complex, tissue engineered structures by inducing undesired differentiation of supporting stem and progenitor cells [1]. Tissue engineered microvessels formed by co-cultures of ECs with SMCs possess lumen and attain EC quiescence, mimicking aspects of physiological microvessels [27, 29].

Biologically-derived gels, such as Matrigel™ and collagen, have been used in the majority of studies of 3D EPC and EC microvessel formation [9]. These gels are usually animal-derived, raising concerns for clinical translation due to immunogenicity issues [30]. In addition, the composition of the extracellular matrix varies widely across tissues with varying amounts of structural proteins such as collagen, elastin, and fibronectin [31]. As well, there exist differences in the composition of bioactive molecules sequestered within the matrix such as growth factors, cytokines, and matrix proteases [31]. These differences may have a significant effect on the differentiation of EPCs towards tissue niche-specific microvasculature. Thus, while the use of biologically-derived gels such as collagen may offer the appropriate cues to initiate microvessel formation, the lack of control over spatial and temporal presentation of bioactive cues limits its application for developing niche-specific tissue microvasculature.

An alternative is the use of bioinspired, synthetic biomaterial systems such as peptide-modified poly(ethylene glycol) (PEG) hydrogels. PEG hydrogels are highly resistant to protein adsorption and thus can serve as an essentially inert, "blank slate" into which one can incorporate biochemical cues to regulate the microvessel formation [32–35]. Specifically, encapsulation of HUVECs and 10T1/2 pericyte progenitor cells within a 3D, matrix metalloproteinase (MMP)-degradable PEG hydrogel system containing the adhesive peptide ligand, RGDS, and VEGF supported robust microvessel formation that was stable for at least 1 month *in vitro*, contained lumen, demonstrated pericyte-localization, and basement membrane deposition [11]. MMP-degradable PEG hydrogels containing VEGF

also supported angiogenesis of microvessels *in vivo* [11, 36] and increased the rate of reperfusion in ischemic tissue [36]. As well, the bioactive molecules within these PEG hydrogel systems can be patterned to mimic the endogenous microvascular structures, such as the cerebral cortex, by controlling their crosslinking with two-photon laser scanning lithography [37].

Incorporation of blood-derived EPCs in favor of vascular-derived ECs within PEG hydrogel systems can further enhance the ability to engineer niche-specific microvasculature. The differentiation potential of EPCs, combined with the capacity of PEG hydrogel systems to mimic endogenous matrices, enables the development of custom modular microvascular units, which could be incorporated into larger tissue-mimetic constructs, aiding efforts to develop vascularized tissue-engineered organs. In the present study, we aimed to establish initial hydrogel and co-culture parameters that support 3D microvessel formation by hCB-EPCs within a PEG hydrogel-based reductionist system. We assessed our success based on the following parameters of physiological microvasculature: lumen formation within microvessels, expression of EC junctional and anti-thrombotic associated proteins, arrest of continued EPC proliferation, perivascular localization by SMCs, basement membrane formation, and stability of microvessel structures for at least 1 month *in vitro*.

Materials & Methods

Isolation of EPCs

Umbilical cord blood was obtained from the Carolina Cord Blood Bank through exempt status by the Institutional Review Board at Duke University. Cord blood was diluted with Hank's Balanced Salt Solution (HBSS) (Gibco®, Life Technologies) at a 1:1 ratio and carefully layered atop Histopaque-1077 (Sigma-Aldrich) solution. The resulting blood/HBSS mixture was separated into erythrocyte, mononuclear cell (MNC), and plasma layers through centrifugation at 740 x g as previously described [17] and plated at 80 x 10^6 cells/cm^2 in 6-well plates coated with 8 μg/cm^2 of rat tail collagen I (BD Biosciences). EPC colonies were isolated 2 weeks after initial plating with clonal isolation rings (Corning). To aid in the isolation of a highly proliferative population of endothelial colony forming cells, EPCs were expanded from primary culture at <400 cells/cm^2 upon tissue culture flasks coated with 8 μg/cm^2 of rat tail collagen I. EPCs were expanded in EBM-2 media (Lonza) containing the EGM-2 bullet kit (Lonza) which includes human vascular endothelial growth factor 165, human basic fibroblastic growth factor (hFGF-B), ascorbic acid, human epidermal growth factor (hEGF), heparin, hydrocortisone, human insulin-like growth factor-1, and gentamycin. Fetal bovine serum (FBS, Atlanta Biologics) and penicillin-streptomycin-amphotericin (abbreviated as penicillin-streptomycin, Invitrogen, 100x concentration solution containing 10,000 U/ml of penicillin, 10,000 μg/ml of streptomycin, 25 μg/ml of amphotericin) were added at 9% v/v and 0.9% v/v, respectively.

Characterization of EPCs

Endothelial outgrowth cells from EPCs were analyzed using flow cytometry with antibodies preconjugated to fluorescein isothiocyanate (FITC) or phycoerythrin (PE) for expression of EC-associated markers CD31 (FITC, Biolegend, 2 μl/10^5 cells), CD105 (PE, Biolegend, 2

μl/10^5 cells), CD146 (FITC, Biolegend, 2 μl/10^5 cells), CD309/VEGFR-2 (PE, Biolegend, 5 μl/10^5 cells); hematopoietic stem cell marker CD34 (FITC, Biolegend, 2 μl/10^5 cells); and lack of expression for leukocyte markers CD45 (FITC, Biolegend, 2 μl/10^5 cells), CD115 (PE, Biolegend, 2 μl/10^5 cells) [17] and an MSC/fibroblast marker, CD90 (FITC, Biolegend, 2 μl/10^5 cells). Mouse isotype IgG (FITC and PE, Biolegend, 2 μl/10^5 cells) was used as a control. Further information on sample preparation can be found in S**upplemental Materials**. Positive controls included human monocytes (THP-1, ATCC) for CD14 and CD45; human macrophages, induced from THP-1 monocytes by treatment with 50 μM 2-mercaptoethanol, for CD115; HUVECs (Lonza) for CD31, CD105, CD146, CD309; and human bone marrow-derived MSCs (Lonza) for CD90. EPCs were analyzed with a Canto analyzer (Becton, Dickinson, and Company (BD)) with a minimum of 9000 events processed per marker. If the EPCs did not express >90% of CD31 or expressed >1% for CD115, CD45, or CD90, they were further processed by fluorescently activated cell sorting (FACS) for CD31+/CD115- populations using a BD DiVa analyzer (BD). EPC populations containing >90% expression for CD31 and <1% CD115, CD45, CD90 were used for all experiments.

To further validate the EC identity of hCB-EPCs, we performed immunofluorescence staining for the EC-associated markers vascular endothelial-cadherin (VE-cadherin, Santa Cruz Biotechnology (Santa Cruz), goat polyclonal IgG, 2 μg/ml), von Willebrand factor (vWF, Santa Cruz, mouse monoclonal IgG1, 2 μg/ml), and endothelial nitric oxide synthase (eNOS, Santa Cruz, rabbit polyclonal IgG, 2 μg/ml). hCB-EPCs were plated onto 8-well coverglass chamber slides (Nunc™ Lab-tek™, 1.5 borosilicate coverglass, Thermo Scientific) at 4 x 10^4 cells/cm^2 and cultured until confluence. hCB-EPCs were fixed with 4% paraformaldehyde for 10 minutes and incubated overnight at 4°C with 3.5% bovine serum albumin (BSA, Fisher BioReagents™) diluted in phosphate buffered saline (PBS) that did not contain calcium or magnesium (Invitrogen). The cultures were then rinsed with PBS and incubated with primary antibodies described above in 3.5% BSA, all at concentrations of 2 μg/ml, and incubated overnight at 4°C. Samples were then rinsed twice (2 hr per rinse) with PBS containing 0.01% Tween 20 (Sigma-Aldrich) and once with PBS. The cells were next incubated with 10 μg/ml of secondary antibodies conjugated to Alexa Fluor® 488 (Invitrogen, donkey anti-goat IgG, for VE-cadherin), Alexa Fluor® 555 (Invitrogen, donkey anti-mouse IgG, for vWF), or Alexa Fluor® 647 (Invitrogen, donkey anti-rabbit IgG, for eNOS) overnight at 4°C. To visualize nuclei, the samples were rinsed with PBS and then stained with 5 μg/ml of 4′,6-diamidino-2-phenylindole (DAPI, Life Technologies) for 1 hr. The samples were rinsed a final time with PBS for 2 hr. Images were taken on a Leica Sp5 confocal microscope at 40x magnification with a numerical aperture of 1.25. The images were collected at 1024 x 1024 pixels with a line and frame scanning average of 2. Sequential scanning was performed to prevent bleed-through of fluorescence. A depth of 12 μm was taken with 1 μm slices for each image.

To characterize network formation potential of hCB-EPCs, we used a Matrigel™ network formation assay (Standard formulation, Corning) as previously described [38]. hCB-EPCs or HUVECs (passage 3), were plated at 4x10^5 cells/cm^2 atop 10 μl Matrigel aliquots within micro-slides for angiogenesis assays (μ–Slides Angiogenesis, ibidi). The media consisted of

EBM-2 containing 2% v/v FBS and 1% v/v penicillin streptomycin without the addition of the EGM-2 bullet kit. Images were taken 18–19 hrs post-plating with an Axiovert 135 inverted microscope (Zeiss) under phase-contrast, and quantified using ImageJ software to assess the number of branch points and total vessel segment length. A branch point was defined as the point of connection between two or more segments. A segment was defined as elongated EC structures, greater than 50 μm in length and between 10–100 μm in thickness.

Cell culture

After validation of their EC phenotype, hCB-EPCs were expanded on collagen-1 coated tissue culture flasks (8 μg/cm^2) at 6.7 x 10^3 cells/cm^2 in EBM-2 media containing EGM-2 supplements, 9% v/v FBS, and 0.9% v/v penicillin-streptomycin. hCB-EPCs from a minimum of 3 separate donors were used between passages 3–5 for all experiments. HUVECs from pooled donors served as an angiogenic EC control [39–40]. HUVECs were cultured in EBM-2 media containing EGM-2 supplements, 2% v/v FBS, and 1% v/v penicillin-streptomycin. HUVECs were plated at 6.7 x 10^3 cells/cm^2 upon tissue culture flasks pre-coated with 8 μg/cm^2 of collagen I and used between passages 3–5 for all experiments. Human monocytes, used as flow cytometry controls for CD14 and CD115, were cultured in RPMI 1640 media containing glucose, L-glutamine, 10% v/v of FBS, 1% v/v penicillin-streptomycin, and 50 μM 2-mercaptoethanol. To induce macrophage differentiation, phorbol myristate acetate (Santa Cruz) was added to the monocyte culture media at a concentration of 320 nM, and added to monocytes (1.33 x 10^4 cells/cm^2) for 48 hr. Human bone marrow-derived MSCs (Lonza), used as a CD90 positive control in flow cytometry analysis, were cultured in DMEM media containing 4.5 g/L glucose, L-glutamine, sodium pyruvate, 10% v/v FBS and 1% v/v penicillin-streptomycin. Human aortic smooth muscle cells (SMCs) (Lonza) were used as a mural cell source to support microvessel formation of HUVECs and hCB-EPCs [22, 25–29]. SMCs were cultured in SmBM media (Lonza) containing SmGM-2 aliquots (insulin, hFGF-B, hEGF, Lonza) and 4.7% v/v FBS, 0.9% v/v penicillin-streptomycin. SMCs were confirmed for mural cell phenotype [6] through immunofluorescence staining for α-SMA (Abcam, mouse monoclonal IgG2a, 1:100 dilution), calponin (Abcam. rabbit monoclonal IgG, 1:100 dilution), PDGFR-β (Santa Cruz, rabbit polyclonal IgG, 1:100 dilution), and ephrin-B2 (Abcam, rabbit polyclonal IgG, 1:100 dilution) using a protocol identical to EPC characterization. SMCs were used between passages 6–9 for all experiments.

2D Network Formation Assay

To aid in visualization of microvessel formation, cells were transduced with fluorescent proteins using a lentiviral system comprised of packaging vectors psPAX2 (Addgene) and PMD2G (Addgene) [26]. The vector FUGW was used for GFP expression. FU tdTomato.W was also produced by replacing the GFP gene in FUGW through simple ligation as previously described [26]. We have shown previously that transduction of hCB-EPCs by these lentiviruses does not affect their network formation potential [27, 38].

EPCs or HUVECs were mixed with SMCs at a 1:4 ratio and seeded atop uncoated, 8-well chambers [26–27, 38]. The total cell number was 1.28 x 10^5 cells/cm^2. Co-culture media

consisted of EBM-2 media containing 9% v/v FBS and 0.9% v/v penicillin-streptomycin. The resulting capillary-like networks were imaged with an Axiovert 135 microscope (Zeiss) at 7 and 14 days after initial plating using red and FITC filters (excitation/emission 546/590 and 450/515, respectively). The networks were quantified using Metamorph® Angiogenesis Tube Formation Application software (Molecular Devices) for total tube length, number of branch points, and average tube thickness. The maximum and minimum width for an endothelial segment to be considered as a microvessel structure was determined by manual adjustment until the range of maximum and minimum values could accurately account for networks within all images. The minimum width was 13.1 μm and the maximum width 100 μm.

RGDS Conjugation to PEG

RGDS (American Peptide) was dissolved in anhydrous dimethyl sulfoxide (DMSO, Sigma) and reacted with acrylate-PEG-succinimidyl valerate (Acryl-PEG-SVA, 3.4 kDa, Laysan Bio), at a 2:1 molar ratio of RGDS to Acryl-PEG-SVA, as previously described [41] (Figure 1A). N,N-diisopropylethylamine (DIPEA, Sigma), added at a 2:1 molar ratio DIPEA to Acryl-PEG-SVA, served as a base. The solution was reacted under argon with rocking. Acryl-PEG-RGDS was purified through dialysis with a 3.5 kDa molecular weight cut-off (MWCO) regenerated cellulose membrane (Spectra/Por®7, Spectrum Labs) against ultrapure water, lyophilized, and analyzed using gel permeation chromatography (GPC) (Polymer Laboratories). To prepare for GPC analysis, samples were dissolved in 0.1% ammonium acetate in N,N-Dimethylformamide (DMF, Sigma) at a concentration of 2 mg/ml, pumped through a polystyrene/divinylbenzene matrix (PLgel column, 5 μm porosity, 500 Å pore size, Polymer Laboratories), and analyzed with an evaporative light scattering (ELS) detector. Conjugation success of RGDS was based on separation of elution peaks between Acryl-PEG-RGDS and Acryl-PEG-SVA. Products with >88% conjugation were used for experiments. The molecular weight of Acryl-PEG-RGDS was near its expected value of 3718 Da, determined through matrix-assisted laser desorption ionization mass spectrometry (Applied Biosystems, DE-Pro Maldi-MS).

MMP-Sensitive Peptide (PQ) Synthesis and Conjugation to PEG

An MMP-2 and -9-sensitive peptide sequence GGGPQG↓IWGQGK (abbreviated as “PQ”, where ↓ denotes the cleavage site) [40], was synthesized using an automated peptide synthesizer (Apex 396, Aapptec) via standard Fmoc chemistry. The final product was cleaved from resin with 95% trifluoroacetic acid and 2.5% triisopropysilane and precipitated in ether. The resulting peptide was dried under vacuum for 1–2 days and its expected molecular weight of 1141 Da confirmed through Maldi-MS.

The PQ peptide was dissolved in anhydrous DMSO (Sigma) and reacted with 3.4 kDa Acryl-PEG-SVA at 1 to 2.1 molar ratio under identical methods as RGDS conjugation to PEG. The lysine group on the PQ peptide enabled conjugation with Acryl-PEG on both the N- and C-terminus to form Acryl-PEG-PQ-PEG-Acryl (abbreviated “PEG-PQ”) as depicted in Figure 1B. The PEG-PQ polymer was purified through dialysis against a 3.5 kDa MWCO regenerated cellulose membrane with ultrapure water over 48 hr with 4 changes of water,

spaced a minimum of 2 hr apart. The purified product was lyophilized and analyzed by GPC as described above. Products with >90% conjugation were used for experiments.

Preparation and Characterization of PEG-PQ + PEG-RGDS Hydrogels

Glass coverslips (12 mm round, no. 1.5, Piranha etched) were first modified with methacrylate groups by reaction with 85 mM 3-(trimethoxysilyl)propyl methacrylate in ethanol for 48 hr to enable attachment of the hydrogels to glass coverslips for easier handling. Hydrogels were formed by dissolving PEG-PQ in PBS (20% w/v) and PEG-RGDS in PBS (5% w/v). The polymer solutions were sterilized by filtration through a 0.22 μm syringe filter and combined with a sterilized photoinitiator solution (0.11 M triethanolamine (TeOA) with 0.02 mM eosin Y, and 9.4 M 1-vinyl-2 pyrrolidinone (NVP) [43] for final concentrations of 6 mM PQ, 3.5 mM RGDS, 50 mM TeOA, 10 μM eosin Y, and 31.7 nM NVP. The polymer solution was pipetted in 5 μl droplets on a Sigmacoted glass slide with 380 μm-thick poly(dimethylsiloxane) (PDMS) spacers. A methacrylate-modified coverslip was placed atop the polymer droplet and clamped to the spacers. Hydrogels were formed by exposure to white light at 120 mW/cm^2 for 40 s (Fiber-lite high intensity illuminator, series 180, Dolan-Jenner Industries, Inc.). The coverslips with the covalently bound hydrogels were transferred to ultra-low adhesion 24-well plates (Corning) and allowed to swell in PBS for a minimum of 8 hr at 37°C before characterization studies.

The mechanical properties of the hydrogels was assessed through compression testing with the Micro-strain analyzer (TA Instruments RSA III) under the Transient, Multiple Extension Mode. Hydrogels were formed using 1 mm thick PDMS spacers and compressed at a rate of 0.002 mm/s. The compressive moduli was obtained from the slope of the linear part of the stress-strain curve.

3D hCB-EPC Network Formation Assay

Co-cultures of EPCs or HUVECs with SMCs were encapsulated within the PEG-PQ hydrogel system by resuspending cell pellets containing 4:1, 1:1, or 1:4 EPC or EC to SMC within the pre-polymer solution described above, at a total cell density of 30 x 10^6 cells/ml (Figure 1C). A monoculture of EPCs at the same density as the 4:1 EC to SMC (24 x 10^6 ECs/ml) served as a control for the effects of the mural cells. The cell-laden hydrogels were placed into 24-well ultra-low adhesion plates (Corning) and supplemented with co-culture media. Media was changed within 24 hr of encapsulation and every 48 hr thereafter.

To visualize microvascular structures within the hydrogels, GFP and tomato-transduced HUVEC or EPC microvessels were assessed 14 days after encapsulation with a multiphoton confocal microscope (Olympus FV1000 Multiphoton). Images were taken using a 25x objective (numerical aperture 1.05) at 150 μm depth with 0.8 μm sections, 1024 x 1024 pixels, line and frame average of 4, and scan speed of 2 μs/pixel. To quantify microvessel formation, hydrogels containing GFP and tomato-transduced HUVECs or EPCs were imaged at 7, 14, and 30 days post-encapsulation with an inverted confocal microscope (Leica DMI6000CS). Images were taken at 10x objective (numerical aperture of 0.4), 60 μm depth from the hydrogel surface with 5 μm thick sections, 1024 x 1024 pixels, with a line and frame average of 2. The images were compiled using Imaris software (Bitplane) and

analyzed with Metamorph® Angiogenesis Tube Formation Application software for total tube length, number of branch points, and average tube thickness using minimum and maximum tube thickness parameters of 10 μm and 100 μm, respectively.

Proliferation Assay

hCB-EPC proliferation within 3D networks was measured at 7, 14, and 22 days after encapsulation through the incorporation of 5-ethynyl-2′-deoxyuridine (EdU) into the DNA of dividing cells (Click-iT® Plus EdU Alexa Fluor® imaging kit, Life Technologies). This imaging kit is compatible with cells that express or are labeled with fluorescent molecules, allowing discrimination between proliferating cells within microvascular networks or behaving as individual cells within 3D co-cultures. At each time point, EdU was added to hydrogels by replacing half of the cell culture media with EdU labeling solution at a final concentration of 10 μM. After 2 hr of incubation at 37°C with 5% CO_2, the cell-laden hydrogels were fixed with 4% v/v formaldehyde (Electron Microscopy Sciences), diluted in PBS, for 15 minutes, rinsed twice with 3% w/v BSA in PBS, and then cells permeabilized for 20 min with 0.5% v/v Triton-X in PBS. The EdU was detected through incubation of samples for 30 min with the Click-iT® EdU buffer which contained picolyl azide functionalized with Alexa Fluor® 488 dye, which reacts with the EdU alkyne group. To detect all nuclei, the samples were rinsed with 3% BSA and incubated with Hoescht® 33342 for 30 min. Samples were imaged with an inverted confocal microscope (Leica) under identical conditions as described for the 3D network quantification. Sequential scanning was performed to prevent bleed-through between channels. The images were compiled in Imaris software (Bitplane) and analyzed in 387.5 μm x 387.5 μm sections with the cell counter tool in ImageJ software.

3D hCB-EPC networks were further characterized for aspects of physiological microvessel formation through immunofluorescent staining after 14 days of culture. Samples were fixed in 3.7% formaldehyde for 10 min, rinsed twice with PBS, and permeabilized with 0.025% v/v Triton-X in PBS for 45 min on a rocker at low speed. The samples were rinsed with 3.5% w/v BSA in PBS for 5 min on the rocker for a total of 3 rinse cycles. The samples were incubated with 3.5% BSA overnight to help reduce nonspecific binding of antibodies. The samples were incubated with the following primary antibodies, diluted with 3.5% BSA, for 48 hr at 4°C on a rocker at low speed: VE-cadherin (Santa Cruz, goat polyclonal IgG, 2 μg/ml), connexin 32 (Abcam, rabbit polyclonal IgG, 10 μg/ml), eNOS (Santa Cruz, rabbit polyclonal IgG, 2 μg/ml), PDGFR-β (Santa Cruz, rabbit polyclonal IgG, 2 μg/ml), α-SMA (Abcam, mouse monoclonal IgG2a, 1:100 dilution), collagen IV (Abcam, mouse monoclonal IgG1, 1:200 dilution), laminin (Abcam, rabbit polyclonal IgG, 1:200 dilution). Samples were rinsed twice with PBS containing 0.01% Tween (Tween® 20, Sigma-Aldrich) and once with PBS. Each rinse cycle lasted a minimum of 4 hr at 4°C on a rocker at low speed. The samples were incubated with secondary antibodies labeled with Alexa Fluor® 488, 555, or 647 (Invitrogen) corresponding to the appropriate host species for the primary antibodies, as described above, at 1:200 dilution for 48 hr at 4°C on a rocker at low speed. To visualize nuclei, the samples were rinsed with PBS before incubation with 5 μg/ml of DAPI (Life Technologies) for 1 hr. The samples were rinsed a final time with PBS for 2 hr and stored in PBS before imaging.

Images were taken on a Leica Sp5 confocal microscope using either 40x (numerical aperture of 1.25) or 63x (numerical aperture of 1.20) objectives. The images were collected at 1024 x 1024 pixels with a line and frame scanning average between 2–6. Sequential scanning was employed to prevent overlap of fluorescence signals. Image depths up to 30 μm were taken with ≤ 1 μm section thicknesses.

Statistics

Statistical analysis on network formation potential of hCB-EPCs in comparison to HUVECs was performed for the Matrigel™ assay using a one-factor analysis of variance (ANOVA) followed by a post-hoc Tukey honest significant difference (HSD) test. The co-culture network formation assay used a two-factor ANOVA followed by a post-hoc Tukey HSD test to examine the effect of EC type and culture period on microvessel formation. The effect of co-culture ratio, EC type, and culture period on 3D microvessel formation within PEG hydrogels was performed with a three-factor ANOVA followed by a post-hoc Tukey HSD test for multiple comparisons. Differences in hCB-EPC proliferation within hydrogels over time was determined with a one-factor ANOVA, followed by a post-hoc Tukey HSD test. JMP® statistics software (SAS) was used for all analysis.

Results

Blood-derived EPCs possess similar phenotype and network formation potential as vascular-derived ECs

Prior to study of microvessel formation within the PEG hydrogels, hCB-EPCs were characterized for EC phenotype and network formation potential. HUVECs have angiogenic potential *in vivo* and *in vitro* [39–40], rendering them an appropriate EC type for comparison in this study. We tested the hypothesis that blood-derived EPCs possessed similar EC phenotype and angiogenic potential as HUVECs by comparing EC protein expression, evaluated with flow cytometry, immunofluorescence, and network formation assays, respectively.

We found hCB-EPCs possessed similar phenotype as HUVECs based on expression of surface antigens associated with ECs (>90% positive for CD31, CD105, CD146, >30% positive for VEGFR2) (Supplemental Figure 1). The hCB-EPCs also contained hematopoietic progenitor cell marker expression (>10% positive for CD34), and lacked expression of leukocyte-associated markers (<1% for CD45, CD115) MSC/fibroblast-associated marker (<1% for CD90). In addition, hCB-EPCs showed similar expression as HUVECs for EC-associated proteins VE-cadherin, vWF, and eNOS (Figure 2A). hCB-EPCs displayed similar potential to form microvessel structures as HUVECs based on the lack of significant differences in total tubule length (p=0.40) of networks formed upon Matrigel™ substrates (Figure 2B–C). We also employed a second network formation assay, utilizing angiogenic mural cells in place of the Matrigel™ substrate [38] (Figure 3). This assay enables observation of microvessel formation within a more physiological setting than Matrigel™ assay and extends the observation period from 24 h to over two weeks of culture [26–27, 38]. The SMCs were confirmed for use as a mural cell source through their expression of α-SMA, calponin, PDGFR-β, and ephrin-B2 (Supplemental Figure 2). By 2

weeks of co-culture, the hCB-EPC networks had significantly greater total tubule length (p=0.03) and connectivity, demonstrated through number of branch points (p=0.006) than HUVEC networks (Figure 3A–C). The average tubule thickness was similar for both HUVECs and EPCs (p=0.66).

MMP-sensitive PEG Hydrogels Support 3D Microvessel Formation by hCB-EPCs

Extension of EPC microvessel formation into a 3D hydrogel scaffold could provide a more biomimetic environment and represent a potentially clinically translatable system. Matrix metalloproteinases (MMPs) are the key proteins for degrading the ECM during angiogenesis, regulating microvessel formation by uncovering new ECM adhesive sites that activate ECs towards an angiogenic phenotype, as well as creating protease byproducts that can inhibit angiogenesis [44–46]. We investigated the ability of PEG hydrogels containing an MMP-sensitive peptide sequence and RGDS to provide the appropriate degradative and adhesive cues to support 3D microvessel formation by hCB-EPCs in co-culture with SMCs. We synthesized and incorporated an MMP2 and 9-sensitive peptide sequence, GGGPQG↓IWGQGK (abbreviated as “PQ”) [42], into PEG by reacting the PQ peptide with Acryl-PEG-SVA (Figure 1B). The product has a PEG-acrylate added to the N-terminus and to the amine group on the lysine at the C-terminus, generating a PEG-diacrylate derivative that can be crosslinked to form a hydrogel. PEG-RGDS is grafted into this hydrogel on a PEG-monoacrylate chain to allow optimal interaction with cell surface receptors. The resulting hydrogels contained 3.5 mM PEG-RGDS and 6 mM PEG-PQ, with a compressive modulus of 18 ± 5 kPa. ECs and SMCs were resuspended in the polymer solution and encapsulated within the hydrogel through cross-linking of PEG-PQ chains upon exposure to visible light in the presence of cytocompatible photoinitiators (Figure 1C).

Intermediate Co-Culture Ratios of hCB-EPCs to SMCs Favor 3D Microvessel Formation

Forming microvessels within a 3D system is more complex than 2D systems because it requires the additional step of cell-mediated gel degradation to enable cell spreading, migration, and ECM deposition. Thus, different EC to SMC ratios may be required for microvessel formation in the 3D system than the 1:4 ratio previously employed in 2D systems [26–27, 38]. We tested EC to SMC ratios of 4:1, 1:1, and 1:4, keeping total cell number constant, and evaluated effects on microvessel morphology by comparing total tubule length, branch points, and average tubule thickness during the first 14 days of culture. The synthetic hydrogel system supported microvessel formation by hCB-EPCs, as well as HUVECs, when combined with SMCs by two weeks of culture (Figure 4A). The majority of microvessel structures resulting from HUVECs and hCB-EPCs were found within 50 μm-depths from the gel surface, with microvessel invasion extending at least 150 μm from the surface (Supplemental Figure 3A). An EC to SMC co-culture ratio of 1:1 best supported microvessel formation by hCB-EPCs, determined by significantly higher total tubule lengths than the 1:4 (p=0.0003) and 4:1 (p=0.0004) ratios after 14 days of culture (Figure 4A). The presence of SMCs was required to support EC microvessel formation within the 3D synthetic hydrogel systems, inferred by the lack of microvessels formed in hCB-EPC monoculture controls (Supplemental Figure 3B–C), which is consistent with previous findings [26–27, 38]. hCB-EPC microvessels were also more connected in the 1:1 co-culture ratio shown by significantly higher amounts of branch points than the 1:4 (p=0.002) and 4:1

(p=0.006) ratios (Figure 4B). hCB-EPC microvessel structures in the 1:1 ratio were stable, indicated by a lack of significant decreases in total tubule length (p=0.79) between days 7 and 14 of culture. A similar trend was observed with microvessel formation by HUVECs (Figure 4A–B). The morphology of hCB-EPC microvessels was similar to that of HUVEC microvessels, by 2 weeks of culture, at the 1:1 co-culture ratio, based on a lack of significant differences in total tubule length (p=1.00), branch points (p=1.00), and average tubule thickness (p=0.06). Increasing the EC to SMC ratio to 4:1 resulted in clustering of ECs rather than microvessel formation (Figure 4A). HUVECs were able to form microvessels at all EC:SMC ratios tested. While there existed some clusters of HUVECs in the 4:1 ratio co-culture condition, there was evidence of microvessel formation, with no significant differences observed in total tubule length ($p > 0.22$), number of branch points ($p > 0.73$), or average tubule thickness ($p > 0.99$) in comparison to the 1:1 and 1:4 ratios, by 14 days of culture. The hCB-EPC microvessels were observable for at least 30 days of *in vitro* culture (Supplemental Figure 3D). Taken together, these observations demonstrate that 3D PEG hydrogels containing an MMP-sensitive peptide and RGDS can support robust formation of stable hCB-EPC microvessels from co-culture with SMCs.

hCB-EPC Microvessels Formed within Synthetic Hydrogels In Vitro Contain Features of In Vivo Physiological Microvasculature

To prepare for anastomosis with the host circulatory system, tissue engineered microvessels must contain lumen and express junctional proteins associated with maintaining permeability and anti-thrombotic function of the vasculature [47]. As well, the microvessels should demonstrate features of physiological, rather than pathological, microvessel formation by arrest of hCB-EPC proliferation after initial network formation, perivascular localization of mural cells, and the presence of basement membrane adjacent to microvascular structures [48–49].

We characterized the hCB-EPC microvasculature structures for these aspects of physiological microvessel formation and found evidence of lumen formation by day 12 of co-culture, shown through cross-sectional images of microvessels containing hollow, circular structures lined with VE-cadherin positive cells in (Figure 5A). In addition to VE-cadherin, an adherens junctional protein critical to maintaining EC permeability [50], the hCB-EPC microvessels also expressed the gap-junctional protein connexin 32, (Figure 5B) an important component to EC intercellular communication and tube formation [51–52]. As well, the hCB-EPC microvessels expressed eNOS (Figure 5C), which helps prevent thrombosis by discouraging platelet adhesion [53].

To evaluate proliferation of hCB-EPCs within microvessels, we added a thymidine analog that incorporates into the DNA of dividing cells, fluorescently-labeled 5-ethynyl-2′-deoxyuridine (EdU), at 7, 14, and 22 days after encapsulation. hCB-EPCs showed a significant decrease in proliferation (p=0.0002), assessed by number of EdU positive cells, between days 7 (5.8%) and 14 (0.5%) of co-culture with SMCs (Figure 6A–B). This quiescent state of hCB-EPCs within microvessel structures was maintained through 22 days of culture with an average of 0.1% proliferating cells. Providing further evidence of a stable microvascular phenotype, perivascular localization by α-SMA and PDGFR-β expressing

cells, presumably SMCs, as well as deposition of basement membrane proteins laminin and collagen IV was seen adjacent to the hCB-EPC microvessel structures by two weeks of co-culture (Figure 5C–D). These findings indicate PEG hydrogel systems can support 3D microvessel formation by hCB-EPCs and SMC co-cultures that are representative of physiological microvasculature.

Discussion

Endothelial progenitor cells (EPCs) are capable of differentiating into all endothelium types found within the body [54–55]. The use of EPCs derived from umbilical cord blood (hCB-EPCs) [56] could provide significant advances to pro-angiogenic therapies and serve as an EC source to vascularize tissue engineered organs *in vitro*. Development of these pre-vascularized structures *in vitro* could also provide novel insights into mechanisms of vasculogenesis by EPCs. Vasculogenesis of EPCs occurs within a fibronectin-rich provisional matrix that is degradable by cell-secreted MMPs [57–58]. Embryonic mechanical properties, estimated from the chick embryo between days 5.5 and 17 of development, exhibit elastic moduli on the order of 10 kPa [59]. In this study, we evaluated whether synthetic hydrogels comprised of PEG conjugated to bioactive peptides could provide adhesive and degradative cues, similar to those found within the embryonic matrix, to support 3D vasculogenesis of EPCs. To test this aim, we utilized a PEG hydrogel system containing covalently-attached cell adhesive and MMP-degradable peptides, which can support microvessel formation by vascular-derived ECs [11]. Due to the need for mural cells to support EPC microvessel formation [11, 33, 35, 60], we utilized a previously established co-culture system of hCB-EPCs and vascular SMCs [26–27, 35], which can produce robust microvessels stable for several weeks *in vitro*, without the need for exogenous angiogenic cytokines beyond those present in serum. We found that PEG hydrogels with a modulus of 18 kPa containing 3.5 mM RGDS and 6 mM of the MMP-sensitive peptide, GGGPQG↓IWGQGK, could support 3D microvessel formation by hCB-EPCs from a 1:1 co-culture ratio with SMCs by 1 week of culture (Figure 4). The hCB-EPCs showed characteristics of physiological microvessels through the presence of lumen, quiescence (<0.1% proliferating cells) of hCB-EPCs within microvascular structures by 2 weeks of culture, expression of gap junctional protein connexin 32, adherens junctional protein VE-cadherin, and eNOS (Figure 6).

hCB-EPC microvessel formation within a synthetic 3D system has been studied for the past decade [25, 61], beginning with work from Bischoff and colleagues [25] that found polymer constructs composed of poly(L-lactide acid) (PLLA) and poly(glycolic acid) (PGA) support microvessel formation by hCB-EPCs by 2 weeks of co-culture with SMCs. The hCB-EPCs formed lumenized microvessels, demonstrated by CD31+ staining, throughout the 1 mm-thick PLLA/PGA construct [25]. While these results offered a novel translatable system to tissue engineer microvasculature, with greater consistency and safety than biologically-derived gels, the disadvantage with PLLA/PGA scaffold materials is that it interacts with cells solely through adsorbed proteins. The use of PEG-based hydrogels may be a more suitable scaffold system for microvessel tissue engineering due to their potential to dynamically regulate microvessel formation through the release of multiple bioactive peptides. For example, furan containing dexamethasone can undergo sustained release

within a malemide-PEG hydrogel system via a Diels-Alder mediated reaction. When this system is encapsulated within a 3D MSC-laden PEG hydrogel construct, it can serve as a delivery depot, inducing osteogenic differentiation of the surrounding MSCs [62]. These PEG-based technologies would be useful for engineering tissue-specific vascular niches, for example, the bone vascular niche, where spatially-controlled release of angiogenic and osteogenic cytokines may aid in the production of a vascular network well-integrated with osteoblasts.

While these reports demonstrate the exciting potential of synthetic hydrogels to mimic the angiogenic matrix, the incorporation of multiple growth factors will become increasingly complex due to the need of regulating their presentation in a time and space-dependent manner [4, 10]. The results of our study demonstrate a simplistic PEG hydrogel system, containing only degradative and adhesive sites, could enable a self-supportive angiogenic microenvironment produced by vascular progenitor cells. This type of positive-control system can be utilized to screen for the efficacy of more sophisticated PEG hydrogel systems to regulate microvessel formation.

The MMP-sensitive peptide sequence used in this study was derived from substitution of the alanine peptide in the native α1(I) collagen chain oligopeptide, GPQG↓IAGQ, with tryptophan (GPQG↓IWGQ), which significantly enhances its degradation rate by MMP2 and 9 [63]. This peptide has been incorporated into synthetic PEG-based hydrogel systems to support 3D growth by fibroblasts, HUVECs, and MSCs [11, 42–43]. Based on the results of this study, we found 6 mM of this MMP-sensitive peptide conjugated to PEG and incorporated with 3.5 mM of RGDS conjugated to PEG, supports microvessel formation of EPCs within mural cell co-culture. Despite the change from a 2D to a 3D system, the co-culture system of hCB-EPCs and SMCs generated microvessels that were similar in structure, evidenced by network morphology parameters of total tubule length per image area (averages near 12 mm/mm^2 for both 2D and 3D systems), branch points per image area (averages near $103/mm^2$ for 2D and $127/mm^2$ for 3D), and average segment diameter (averages near 35 μm for 2D and 27 μm for 3D) [26–27, 37]. Based on the results of the monoculture of EPCs (Supplemental Figure 3B), the adhesive and protease-sensitive peptides incorporated into PEG do not stimulate microvessel formation, indicating the hydrogel in this study serves a passive role to support interactions of mural cells with EPCs.

The optimal ratio of ECs to stromal cells that supports microvessel formation within PEG-based hydrogels varies among studies from 10:1 to 1:1 [11, 33–34, 64]. We found a 4:1 ratio of ECs to SMCs decreased microvessel formation in comparison to 1:1 ratios, with hCB-EPCs showing more sensitivity to co-culture ratios than HUVECs (Figure 4). Differences in the choice of stromal cells, which include fibroblasts, MSCs, pericytes, and SMCs as well as the composition of culture media, may explain these discrepancies. For example, MSCs best support EC microvessel ratio at ratios greater than 4:1 EC to MSC [33, 65] with pericytes and 10T1/2 mesenchymal progenitor cells also support microvessels at the higher 4:1 EC to stromal cell ratio [11]. In contrast, fibroblasts derived from the human lung and SMCs are most frequently reported to support 3D microvessel formation at 1:1 ratios of ECs to mural cells [34, 64]. As well, the addition of supplemental growth factors in the culture media, such as bFGF and VEGF, may alter the balance of angiogenic cytokines needed to regulate

microvessel formation [54]. A comparison of stromal cell effects on EC microvessel formation under basal media conditions, containing no additional growth factors beyond those present in serum, would assist efforts to reveal the mechanism behind these differences.

One explanation for the ability of HUVECs to form microvessels at all co-culture ratios tested within the 3D hydrogel system in comparison to hCB-EPCs, which only formed microvessels at the 1:1 co-culture ratio, is their microenvironment prior to use in microvessel tissue engineering. The HUVECs function as part of the vasculature, with exposure to blood flow. In contrast, the EPCs are presumed as circulatory cells, with possible origins in the vasa vasorum [66]. These differences in the location of HUVECs and EPCs prior to isolation may allow HUVECs to possess a more differentiated EC phenotype than the EPCs. Perhaps preconditioning the EPCs prior to use in microvessel tissue engineering by exposure to flow could differentiate EPCs towards angiogenic ECs by upregulating the expression of EC proteins associated with angiogenic function.

Although the cells were dispersed throughout the gel at the time of encapsulation, the majority of microvessel growth was limited to the first 50 μm from the gel surface, most likely due to the greater availability of oxygen. Future work testing the mechanical properties of the cell-laden gels throughout the culture period could help characterize this system to determine whether the onset of microvessel formation is correlated with a decrease in the hydrogel's elastic modulus. The thin layer of vascularization is a limitation to our model of EPC microvessel formation (Supplemental Figure 3A). However, this limitation may be overcome by adjusting parameters of the hydrogel and the co-culture. For example, HUVECs and SMCs demonstrated microvessel invasion to depths of at least 1 mm [64]. The reasons for these discrepancies in microvessel invasion depth may be explained by the several fold higher density of cells used in our study as well as the homogeneous cell distribution within the gel at the beginning of culture, rather than the use of spheroid aggregates that are inserted into the bulk hydrogel [64]. As well, the elastic modulus of the hydrogel was 2.13 kPa [64], significantly lower than the elastic modulus of the hydrogel used in our study, which was near 18 kPa. Future work utilizing softer hydrogels and varying seeding density and method of co-culture could result in a thick (>200 μm) vascularized construct, more suitable for translation research with hCB-EPCs.

Applications for this 3D microvessel system include screening drugs for angiogenic therapies, with an emphasis on reducing off-target consequences by comparing drug effects on physiological microvessels to effects on pathological microvessel formation [67]. In addition, this system can serve as a positive control to validate novel biomaterial strategies for directing EPC microvessel formation. Specifically, strategies to promote EPC differentiation towards tissue-specific endothelium. This model could also help stem cell biologists working to integrate iPSCs, or other stem cell sources into microvessels by screening the candidate stem cell's ability to support EPC microvessel formation in comparison to SMCs [26, 38].

Conclusion

The results of this study provide initial parameters to construct PEG-based hydrogels that support EPC microvessel formation. Our system serves as a starting point for the design of custom hydrogels that can support diverse microvascular tissue engineering applications. Future studies may examine alternative forms of adhesive and protease-sensitive peptides to enable EPC network formation from co-culture with parenchymal-specific cells. This novel, reductionist system can also be used to elucidate mechanisms of vasculogenesis by progenitor cells.

Supplementary Material

Refer to Web version on PubMed Central for supplementary material.

Acknowledgments

This study was supported by NIH grant 5R01HL097520 and NSF Graduate Research Fellowship 1106401 to E.B.P. The authors would like to acknowledge Ms. Yan Wu for her assistance in mechanical testing.

References

1. Rouwkema J, Rivron NC, van Blitterswijk CA. Vascularization in tissue engineering. Trends Biotechnol. 2008; 26:434–441. [PubMed: 18585808]
2. Novosel EC, Kleinhans C, Kluger PJ. Vascularization is the key challenge in tissue engineering. Adv Drug Deliv Rev. 2011; 63:300–311. [PubMed: 21396416]
3. Welti J, Loges S, Dimmeler S, Carmeliet P. Recent molecular discoveries in angiogenesis and antiangiognic therapies in cancer. J Clin Invest. 2013; 123:3190–3200. [PubMed: 23908119]
4. Potente M, Gerhardt H, Carmeliet P. Basic and therapeutic aspects of angiogenesis. Cell. 2011; 146:873–887. [PubMed: 21925313]
5. Hirschi KK, Rohovsky SA, Beck LH, Smith SR, D'Amore PA. Endothelial cells modulate the proliferation of mural cell precursors via platelet-derived growth factor-BB and heterotypic cell contact. Circ Res. 1999; 84:298–305. [PubMed: 10024303]
6. Armulik A, Genové G, Betsholtz C. Pericytes: developmental, physiological, and pathological perspectives, problems, and promises. Dev Cell. 2011; 21:193–215. [PubMed: 21839917]
7. Hirschi KK, Burt JM, Hirschi KD, Dai C. Gap junction communication mediates transforming growth factor-beta activation and endothelial-induced mural cell differentiation. Circ Res. 2003; 93:429–437. [PubMed: 12919949]
8. Fang JS, Dai C, Kurjiaka DT, Burt JM, Hirschi KK. Connexin45 regulates endothelial-induced mesenchymal cell differentiation toward a mural cell phenotype. Arterioscler Thromb Vasc Biol. 2013; 33:362–368. [PubMed: 23220276]
9. Kirkpatrick CJ, Fuchs S, Unger RE. Co-culture systems for vascularization—learning from nature. Adv Drug Deliv Rev. 2011; 63:291–299. [PubMed: 21281686]
10. Carmeliet P. Angiogenesis in life, disease, and medicine. Nature. 2005; 438:932–936. [PubMed: 16355210]
11. Moon JJ, Saik JE, Poche RA, Leslie-Barbick JE, Lee S, Smith AA, Dickinson ME, West JL. Biomimetic hydrogels with pro-angiogenic properties. Biomaterials. 2010; 31:3840–3847. [PubMed: 20185173]
12. Tremblay PL, Hudon V, Berthod F, Germain L, Auger FA. Inosculation of tissue-engineered capillaries with the host's vasculature in a reconstructed skin transplanted on mice. Am J Transplant. 2005; 5:1002–1010. [PubMed: 15816880]

13. Chen X, Aledia AS, Ghajar CM, Griffith CK, Putnam AJ, Hughes CC, George SC. Prevascularization of a fibrin-based tissue construct accelerates the formation of functional anastomosis with host vasculature. Tissue Eng Part A. 2009; 15:1363–1371. [PubMed: 18976155]
14. Unger RE, Ghanaati S, Orth C, Sartoris A, Barbeck M, Halstenberg S, Motta A, Migliaresi C, Kirkpatrick CJ. The rapid anastomosis between prevascularized networks on silk fibroin scaffolds generated in vitro with co-cultures of human microvascular endothelial and osteoblast cells and the host vasculature. Biomaterials. 2010; 31:6959–6967. [PubMed: 20619788]
15. Leong MF, Toh JK, Du C, Narayanan K, Lu HF, Lim TC, Wan AC, Ying JY. Patterned prevascularised tissue constructs by assembly of polyelectrolyte hydrogel fibres. Nat Commun. 2013; 4:2353. [PubMed: 23955534]
16. Sekine H, Shimizu T, Hobo K, Sekiya S, Yang J, Yamato M, Kurosawa H, Kobayashi E, Okano T. Endothelial cell co-culture within tissue-engineered cardiomyocyte sheets enhances neovascularization and improves cardiac function of ischemic hearts. Circulation. 2008; 118:S145–S152. [PubMed: 18824746]
17. Ingram DA, Mead LE, Tanaka H, Meade V, Fenoglio A, Mortell K, Pollok K, Ferkowicz MJ, Gilley D, Yoder MC. Identification of a novel hierarchy of endothelial progenitor cells using human peripheral and umbilical cord blood. Blood. 2004; 104:2752–2760. [PubMed: 15226175]
18. Yoder MC. Human endothelial progenitor cells. Cold Spring Harb Perspect Med. 2012; 2:a006692. [PubMed: 22762017]
19. Bompais H, Chagraoui J, Canron X, Crisan M, Liu XH, Anjo A, Tolla-Le Port C, Leboeuf M, Charbord P, Bikfalvi A, Uzan G. Human endothelial cells derived from circulating progenitors display specific functional properties compared with mature vessel wall endothelial cells. Blood. 2004; 103:2577–2584. [PubMed: 14630797]
20. Eapen M, Klein JP, Ruggeri A, et al. Impact of allele-level HLA matching on outcomes after myeloablative single unit umbilical blood transplantation for hematologic malignancy. Blood. 2014; 123:133–140. [PubMed: 24141369]
21. Anagnostakis I, Papassavas AC, Michalopoulos E, Chatzistamatiou T, Andriopoulou S, Tsakris A, Stavropoulos-Giokas C. Successful short-term cryopreservation of volume-reduced cord blood units in a cryogenic mechanical freezer: effects on cell recovery, viability, and clonogenic potential. Transfusion. 2014; 54:211–223. [PubMed: 23692393]
22. Melero-Martin JM, Khan ZA, Picard A, Wu X, Paruchuri S, Bischoff J. In vivo vasculogenic potential of human blood-derived endothelial progenitor cells. Blood. 2007; 109:4761–4768. [PubMed: 17327403]
23. Yang J, Nagavarapu U, Relloma K, Sjaastad MD, Moss WC, Passaniti A, Herron GS. Telomerized human microvasculature is functional in vivo. Nat Biotechnol. 2001; 19:219–224. [PubMed: 11231553]
24. Abdallah BM, Haack-Sørensen M, Burns JS, Elsnab B, Jakob F, Hokland P, Kassem M. Maintenance of differentiation potential of human bone marrow mesenchymal stem cells immortalized by human telomerase reverse transcriptase gene despite [corrected] extensive proliferation. Biochem Biophys Res Commun. 2005; 326:527–538. [PubMed: 15596132]
25. Wu X, Rabkin-Aikawa E, Guleserian KJ, Perry TE, Masuda Y, Sutherland FW, Schoen FJ, Mayer JE Jr, Bischoff J. Tissue-engineered microvessels on three-dimensional biodegradable scaffolds using human endothelial progenitor cells. Am J Physiol Heart Circ Physiol. 2004; 287:H480–487. [PubMed: 15277191]
26. Peters EB, Christoforou N, Moore E, West JL, Truskey GA. CD45+ cells present within mesenchymal stem cell populations affect network formation of blood-derived endothelial outgrowth cells. Biores Open Access. 2015:4.1.10.1089/biores.2014.0029
27. Peters EB, Christoforou N, Leong KW, Truskey GA. Comparison of mixed and lamellar co-culture spatial arrangements for tissue engineering capillary networks in vitro. Tissue Eng Part A. 2013; 19:697–706. [PubMed: 23171167]
28. Evensen L, Micklem DR, Blois A, Berge SV, Aarsaether N, Littlewood-Evans A, Wood J, Lorens JB. Mural cell associated VEGF is required for organotypic vessel formation. PLoS ONE. 2009; 4:e5798. [PubMed: 19495422]

29. Korff T, Kimmina S, Martiny-Baron G, August HG. Blood vessel maturation in a 3-dimensional spheroidal co-culture model: direct contact with smooth muscle cells regulates endothelial cell quiescence and abrogates VEGF responsiveness. FASEB J. 2001; 15:447–457. [PubMed: 11156960]
30. Morais JM, Papadimitrakopoulos F, Burgess DJ. Biomaterials/tissue interactions: Possible solutions to overcome foreign body response. AAPS J. 2010; 12:188–196. [PubMed: 20143194]
31. Minuth, WW.; Strehl, R.; Schumacher, K. Essentials for Daily Laboratory Work. Weinheim: Wiley-VCH Verlag; 2005. Tissue Engineering.
32. Saik JE, Gould DJ, Keswani AH, Dickinson ME, West JL. Biomimetic hydrogels with immobilized ephrinA1 for therapeutic angiogenesis. Biomacromolecules. 2011; 12:2715–2722. [PubMed: 21639150]
33. Chwalek K, Tsurkan MV, Freudenberg U, Werner C. Glycosaminoglycan-based hydrogels to modulate heterocellular communication in in vitro angiogenesis models. Sci Rep. 2014; 4:4414. [PubMed: 24643064]
34. Vigen M, Ceccareli J, Putnam AJ. Protease-sensitive PEG hydrogels regulate vascularization in vitro and in vivo. Macromol Biosci. 2014; 14:1368–1379. [PubMed: 24943402]
35. Seeto WJ, Tian Y, Lipke EA. Peptide-grafted poly(ethylene glycol) hydrogels support dynamic adhesion of endothelial progenitor cells. Acta Biomater. 2013; 9:8279–8289. [PubMed: 23770139]
36. Phelps EA, Landázuri N, Thulé PM, Taylor WR, García AJ. Bioartificial matrices for therapeutic vascularization. Proc Natl Acad Sci USA. 2010; 107:3323–3328. [PubMed: 20080569]
37. Culver JC, Hoffman JC, Poché RA, Slater JH, West JL, Dickinson ME. Three-dimensional biomimetic patterning in hydrogels to guide cellular organization. Adv Mater. 2012; 24:2344–2348. [PubMed: 22467256]
38. Peters EB, Liu B, Christoforou N, West JL, Truskey GA. Umbilical cord blood-derived mononuclear cells exhibit pericyte-like phenotype and support network formation of endothelial progenitor cells in vitro. Ann Biomed Eng. 201510.1007/s10439-015-1301-z
39. Hotchkiss KA, Ashton AW, Mahmood R, Russell RG, Sparano JA, Schwartz EL. Inhibition of endothelial cell function in vitro and angiogenesis in vivo by docetaxel (Taxotere): association with impaired repositioning of the microtubule organizing center. Mol Cancer Ther. 2002; 1:1191–1200. [PubMed: 12479700]
40. Haug V, Torio-Padron N, Stark GB, Finkenzeller G, Strassburg S. Comparison between endothelial progenitor cells and human umbilical vein endothelial cells on neovascularization in an adipogenesis mouse model. Microvasc Res. 2015; 97:159–166. [PubMed: 25446371]
41. Hahn MS, Tate LJ, Moon JJ, Rowland MC, Ruffino KA, West JL. Photolithographic patterning of polyethylene glycol hydrogels. Biomaterials. 2006; 27:2519–2524. [PubMed: 16375965]
42. Lutolf MP, Lauer-Fields JL, Schmoekel HG, Metters AT, Weber FE, Fields GB, Hubbell JA. Synthetic matrix metalloproteinase-sensitive hydrogels for the conduction of tissue regeneration: engineering cell-invasion characteristics. Proc Natl Acad Sci USA. 2003; 100:5413–5418. [PubMed: 12686696]
43. Bahney CS, Lujan TJ, Hsu CW, Bottlang M, West JL, Johnstone B. Visible light photoinitiation of mesenchymal stem cell-laden bioresponsibe hydrogels. Eur Cell Mater. 2011; 22:43–55. [PubMed: 21761391]
44. Stupack DG, Cheresh DA. Integrins and angiogenesis. Curr Top Dev Biol. 2004; 64:207–238. [PubMed: 15563949]
45. Eming SA, Hubbell JA. Extracellular matrix in angiogenesis: dynamic structures with translational potential. Exp Dermatol. 2011; 20:605–613. [PubMed: 21692861]
46. Senger DR, Davis GE. Angiogenesis. Cold Spring Harb Perspect Biol. 2011; 3:a005090. [PubMed: 21807843]
47. Adams RH, Alitalo K. Molecular regulation of angiogenesis and lymphangiogenesis. Nat Rev Mol Cel Biol. 2007; 8:464–478.
48. Belvisi L, Riccioni T, Marcellini M, Vesci L, Chiarucci I, Efrati D, Potenza D, Scolastico C, Manzoni L, Lombardo K, Stasi MA, Orlandi A, Ciucci A, Nico B, Ribatti D, Giannini G, Presta M, Carminati P, Pisano C. Biological and molecular properties of a new alpha(v)beta3/alpha(v)beta5 integrin antagonist. Mol Cancer Ther. 2005; 4:1670–1680. [PubMed: 16275988]

49. Kut C, Mac Gabhann F, Popel AS. Where is VEGF in the body? A meta-analysis of VEGF distribution in cancer. Br J Cancer. 2007; 97:978–985. [PubMed: 17912242]
50. Dejana E, Orsenigo F, Lampugnani MG. The role of adherens junctions and VE-cadherin in control of vascular permeability. J Cell Sci. 2008; 121(Pt 13):2115–2122. [PubMed: 18565824]
51. Okamoto T, Akiyama M, Takeda M, Gabazza EC, Hayashi T, Suzuki K. Connexin32 is expressed in vascular endothelial cells and participates in gap-junction intercellular communication. Biochem Biophys Res Commun. 2009; 382:264–268. [PubMed: 19265674]
52. Okamoto T, Akita N, Kawamoto E, Hayashi T, Suzuki K, Shimaoka M. Endothelial connexin32 enhances angiogenesis by positively regulating tube formation and cell migration. Exp Cell Res. 2014; 321:133–141. [PubMed: 24333598]
53. Tziros C, Freedman JE. The many antithrombotic actions of nitric oxide. Curr Drug Targets. 2006; 7:1243–1251. [PubMed: 17073585]
54. Herbert SP, Stainier DY. Molecular control of endothelial cell behavior during blood vessel morphogenesis. Nat Rev Mol Cell Biol. 2011; 12:551–564. [PubMed: 21860391]
55. Yoder MC. Endothelial progenitor cell: a blood cell by many other names may serve similar functions. J Mol Med (Berl). 2013; 91:285–295. [PubMed: 23371317]
56. Yoder MC, Mead LE, Prater D, Krier TR, Mroueh KN, Li F, Krasich R, Temm CJ, Prchal JT, Ingram DA. Redefining endothelial progenitor cells via clonal analysis and hematopoietic stem/progenitor cell principals. Blood. 2007; 109:1801–1809. [PubMed: 17053059]
57. Senger DR. Molecular framework for angiogenesis: a complex web of interactions between extravasated plasma proteins and endothelial cell proteins induced by angiogenic cytokines. Am J Pathol. 1996; 149:1–7. [PubMed: 8686733]
58. Hynes RO. Cell-matrix adhesion in vascular development. J Thromb Haemost. 2007; 5(Supplement 1):32–40. [PubMed: 17635706]
59. Marturano JE, Arena JD, Schiller ZA, Georgakoudi I, Kuo CK. Characterization of mechanical and biochemical properties of developing embryonic tendon. Proc Natl Acad Sci USA. 2013; 110:6370–6375. [PubMed: 23576745]
60. Jain RK. Molecular regulation of vessel maturation. Nat Med. 2003; 9:685–693. [PubMed: 12778167]
61. Hanjaya-Putra D, Bose V, Shen YI, Yee J, Khetan S, Fox-Talbot K, Steenbergen C, Burdick JA, Gerecht S. Controlled activation of morphogenesis to generate a functional human microvasculature in a synthetic matrix. Blood. 2011; 118:804–815. [PubMed: 21527523]
62. Koehler KC, Alge DL, Anseth KS, Bowman CN. A Diels-Alder modulated approach to control and sustain the release of dexamethasone and induce osteogenic differentiation of human mesenchymal stem cells. Biomaterials. 2013; 34:4150–4158. [PubMed: 23465826]
63. Nagase H, Fields GB. Human matrix metalloproteinase specificity studies using collagen sequence-based synthetic peptides. Biopolymers. 1996; 40:399–416. [PubMed: 8765610]
64. Turturro MV, Christenson MC, Larson JC, Young DA, Brey EM, Papavasiliou G. MMP-sensitive PEG diacrylate hydrogels with spatial variations in matrix properties stimulate directional vascular sprout formation. PLoS. 2013; 8:e58897.
65. Rao RR, Peterson AW, Ceccarelli J, Putnam AJ, Stegemann JP. Matrix composition regulates three-dimensional network formation by endothelial cells and mesenchymal stem cells in collagen/fibrin materials. Angiogenesis. 2012; 15:253–264. [PubMed: 22382584]
66. Kawabe J, Hasebe N. Role of the vasa vasorum and vascular resident stem cells in atherosclerosis. Biomed Res Int. 2014:Article ID 701571, 8.10.1155/2014/701571
67. Gill BJ, Gibbons DL, Roudsari LC, Saik JE, Rizvi ZH, Roybal JD, Kurie JM, West JL. A synthetic matrix with independently tunable biochemistry and mechanical properties to study epithelial morphogenesis and EMT in a lung adenocarcinoma model. Cancer Res. 2012; 72:6013–6023. [PubMed: 22952217]

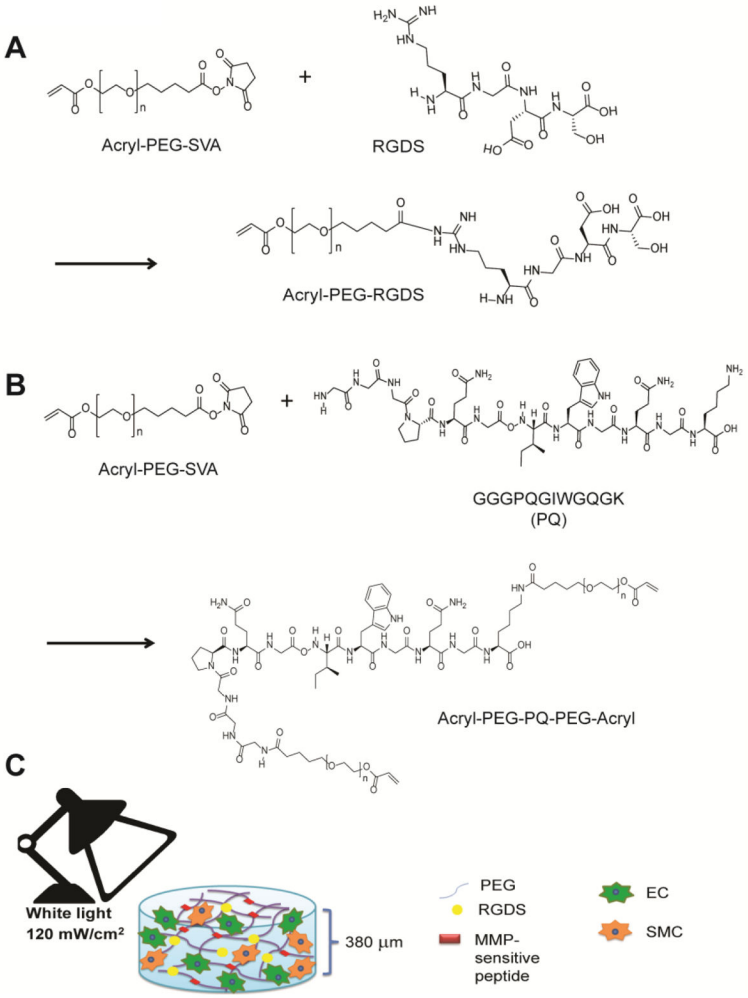

Figure 1. Schematic of 3D PEG hydrogel system to support EPC microvessel formation

(**A**) Overview of acryl-PEG-RGDS (PEG-RGDS) synthesis. (**B**) An MMP-sensitive peptide sequence (PQ) was incorporated into PEG diacrylate (PEGDA) through reaction with Acryl-PEG-SVA at a 1 to 2.1 molar ratio to form Acryl-PEG-PQ-PEG-Acryl (PEG-PQ). (**C**) Co-cultures of ECs with SMCs were mixed with PEG-PQ, PEG-RGDS, and polymerization components eosin Y, triethanolamine, and 1-vinyl-2 pyrrolidinone. Hydrogels were formed from the mixture by exposure under visible light at 120 mW/cm^2 for 40s.

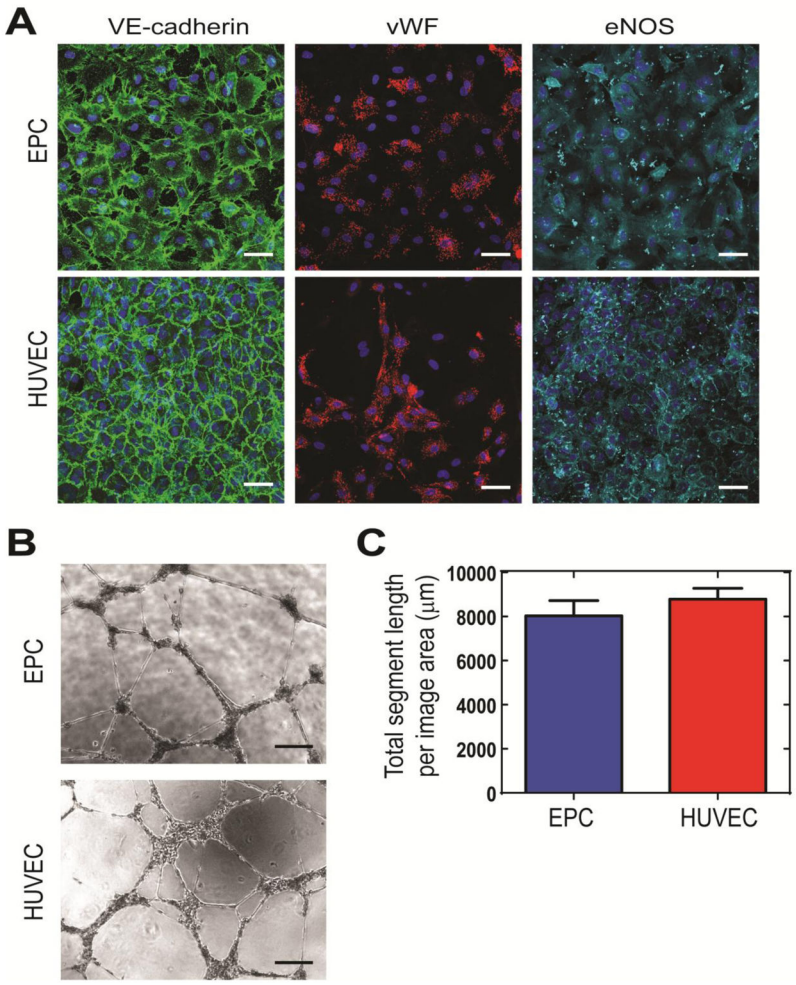

Figure 2. Characterization of umbilical cord blood-derived endothelial progenitor cells (hCB-EPCs)

(**A**) EPCs demonstrate similar expression for VE-cadherin, von Willebrand factor (vWF), and endothelial nitric oxide synthase (eNOS) as human umbilical vein-derived endothelial cells (HUVECs). Nuclei were counterstained with DAPI. Scale bar equals 50 μm. (**B**) Representative images of network formation by EPCs and HUVECs upon Matrigel™ substrates, 18–19 hours post-plating. Scale bar equals 250 μm. (**C**) Comparison of total segment length from Matrigel™ assays between EPCs and HUVECs. Image area analyzed is 2.3 mm^2. *n*=5 images analyzed per condition.

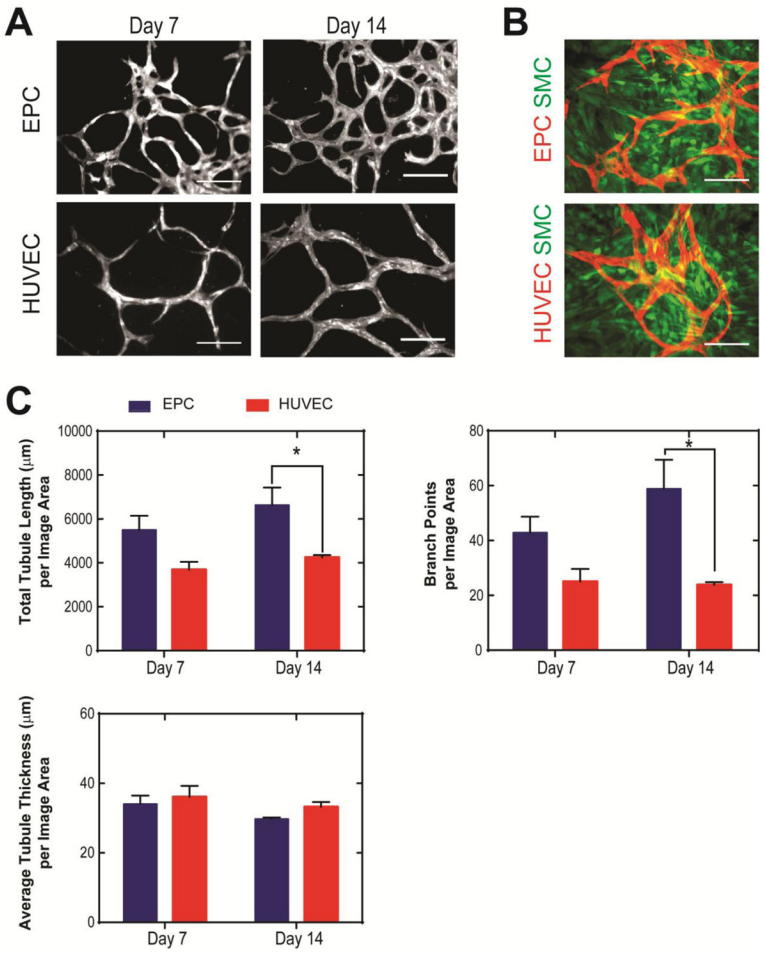

Figure 3. Comparison of network formation by hCB-EPCs and HUVECs upon co-culture with mural cells

(**A**) Representative images of network formation by fluorescent protein-transduced hCB-EPCs (EPCs) and HUVECs in co-culture with SMCs (not visible) at 7 and 14 days after plating tissue-culture treated glass. Scale bar = 200 μm. (**B**) Representative images of SMCs (green) in co-culture with hCB-EPCs and HUVECs (red) after 14 days of culture. Scale bar = 200 μm. (**C**) Quantitative analysis of EPC and HUVEC network morphology during the first 14 days of culture assessed through total tubule length, branch points, and average tubule thickness. * indicates significant difference, $p < 0.05$. n=5–6 images analyzed per condition from 2 separate experiments. Image area analyzed is 0.57 mm^2 per image.

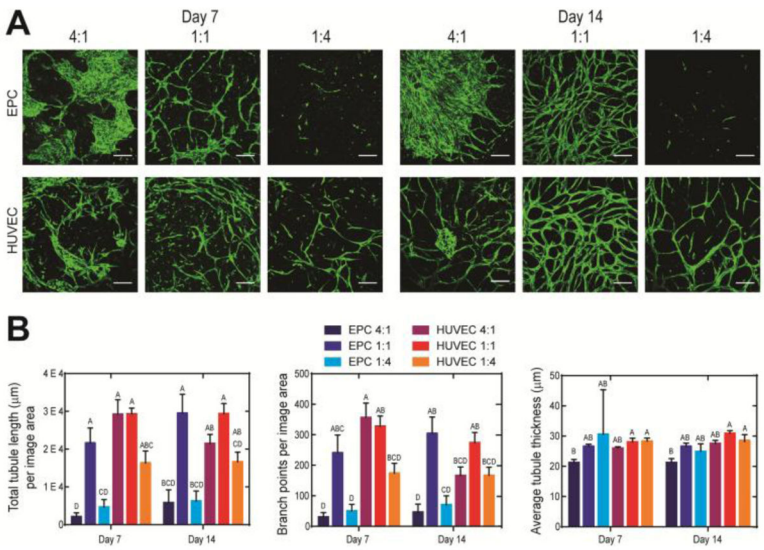

Figure 4. Effect of EC:SMC co-culture ratio upon 3D microvessel formation within a synthetic hydrogel system

(**A**) Representative images of microvessel formation from GFP-transduced HUVECs and hCB-EPCs (EPCs) in 4:1, 1:1, and 1:4 co-culture with SMCs (not visible) during the first 2 weeks of culture. Images were taken within a 50-μm depth from the gel surface. Scale bar equals 250 μm. (**B**) Quantification for differences in total tubule length, branch points, and average tubule thickness in microvessels formed by varying co-culture ratios and use of EPCs or HUVECs at days 7 and 14 of culture. Conditions not connected by the same letter are significantly different. *n*=4–5 images analyzed per condition from a minimum of 2 separate experiments. Image area analyzed is 2.4 mm^2.

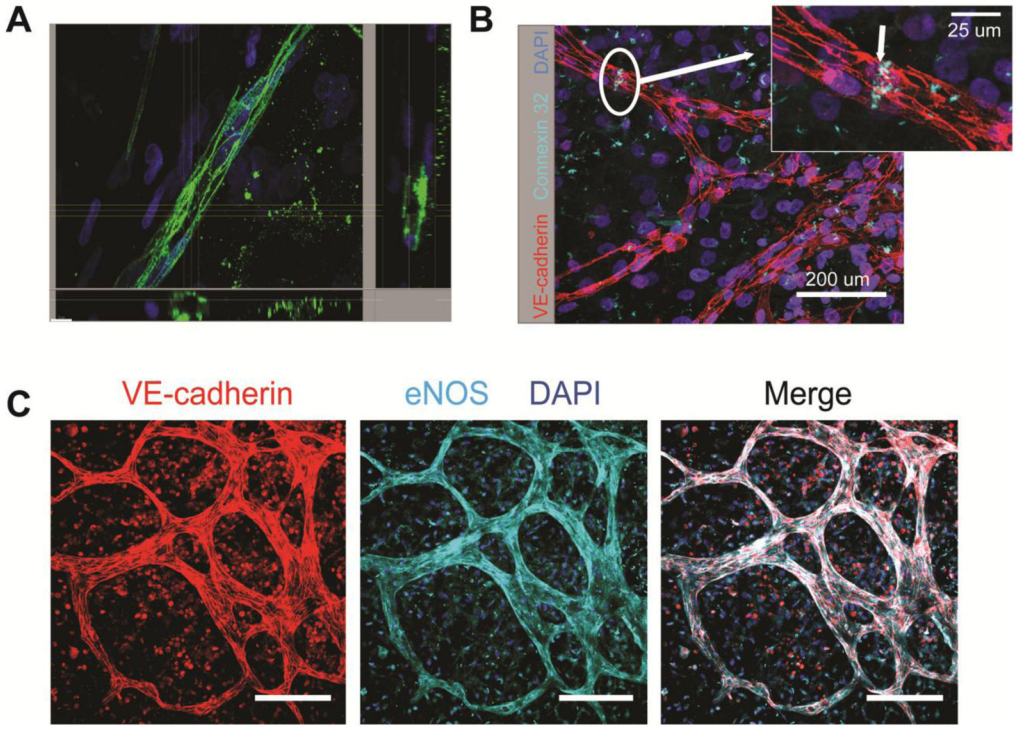

Figure 5. hCB-EPCs within 3D microvessels form lumen and express proteins associated with maintaining permeability and anti-thrombotic function

(**A**) Representative cross-sectional hCB-EPC microvessels, immunostained with VE-cadherin (green), formed after 12 days of co-culture with SMCs. Nuclei are indicated by (DAPI) (blue). Scale bar, located on the bottom left corner, equals 10 μm. (**B**) Representative image hCB-EPC microvessels after 14 days of co-culture with SMCs depicting expression of connexin 32 gap junction (Cyan) between two adjacent hCB-EPCs, identified through VE-cadherin expression (red). Nuclei are depicted through incorporation of DAPI. Scale bar equals 200 μm for the image and 20 μm for the inset. (**C**) Representative images depicting the expression of eNOS localized the hCB-EPC microvessels, formed after 14 days of co-culture with SMCs. Nuclei are shown through incorporation of DAPI. Scale bar equals 100 μm

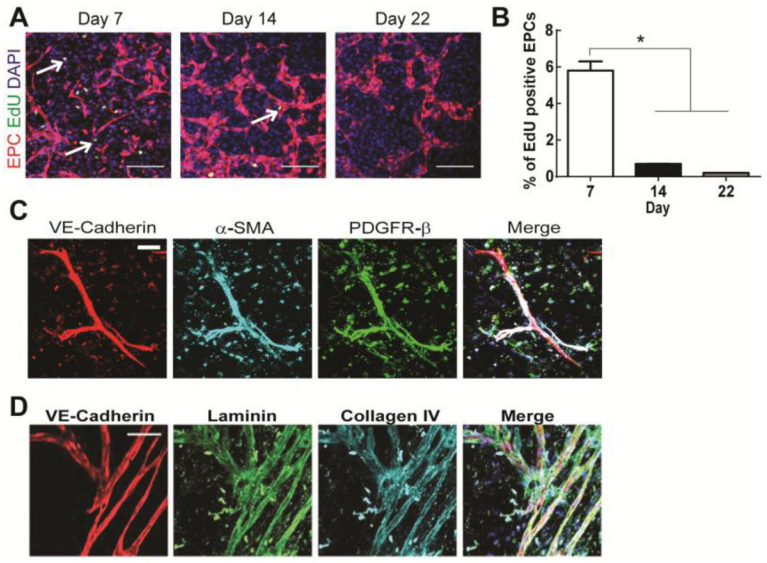

Figure 6. hCB-EPCs in microvessels arrest proliferation by 2 weeks of co-culture with SMCs, contain pericyte investment and basement membrane

(**A**) Representative images of EdU assay analysis on during the first 22 days of hCB-EPC microvessel formation. EdU (green, indicated by white arrows) was incorporated into the DNA of cells and distinguished between cell types with tomato fluorescent protein-transduced hCB-EPCs in co-culture with SMCs (not visible). Nuclei are indicated through DAPI (blue). Scale bar equals 200 μm. (**B**) Quantitative results for hCB-EPC proliferation from the EdU assay. * indicates $p < 0.05$. $n=3$ images analyzed per time point. (**C**) Representative images of hCB-EPC microvessels, after 14 days of co-culture with SMCs, immunostained for pericyte investment based upon expression of α-SMA (cyan), PDGFR-β (green) adjacent to microvessel structures (VE-cadherin, red). Nuclei are indicated with DAPI. Scale bar equals 50 μm. (**D**) Representative images of hCB-EPC microvessels, after 14 days of co-culture with SMCs, immunostained for the presence of basement membrane based upon expression of laminin (green) and collagen IV (cyan) protein deposition adjacent to microvessel structures (VE-cadherin, red). Nuclei are indicated with DAPI. Scale bar equals 100 μm.